Investigation of the Photochemical, Electrochemical, and Spectroelectrochemical Properties of an Iridium(III)/Ruthenium(II) Mixed-Metal Complex Bridged by 2,3,5,6-Tetrakis(2-pyridyl)pyrazine

Lisa M. Vogler, Brian Scott,† and Karen J. Brewer*

Department of Chemistry, Virginia Polytechnic Institute and State University, Blacksburg, Virginia 24061-0212

Received July 24, 1991

The mixed-metal complex $[(tpy)Ru(tpp)IrCl_3]^{2+}$ and the model monometallic fragments $[Ir(tpp)Cl_3]$ and $[Ru(tpy)(tpp)]^{2+}$ have been prepared and their spectroscopic, electrochemical, and spectroelectrochemical properties studied (where tpp = 2,3,5,6-tetrakis(2-pyridyl)pyrazine and tpy = 2,2′:6′,2″-terpyridine). This bimetallic system is the first example of a tpp-bridged mixed-metal complex. The combination of ruthenium, a good light absorber, with iridium, a catalytic metal center, into one molecule is of interest in intramolecular photosensitization schemes. The complex $[Ir(tpp)Cl_3]$ has been crystallized and its structure determined by X-ray crystallography. $[Ir(tpp)Cl_3]$ was found to crystallize in the monoclinic space group $C2/c$, with $a = 8.745(2)$ Å, $b = 21.215(5)$ Å, $c = 17.734(4)$ Å, $\beta = 92.21(2)°$, $V = 3288(1)$ Å^3, $Z = 4$, $d_x = 1.68$, and $R = 0.0433$. The iridium atom sits in a distorted octahedral environment with the three nitrogens of the tpp ligand and a chlorine atom defining the equatorial plane. The axial positions are occupied by chlorine atoms. All three compounds, $[Ir(tpp)Cl_3]$, $[Ru(tpy)(tpp)]^{2+}$, and $[(tpy)Ru(tpp)IrCl_3]^{2+}$, emit in fluid solution at room temperature, and the energy and lifetimes of these luminescences were determined. The mixed-metal system displays properties that are unique from either of the monometallic complexes with lower energy absorptions and emission, as well as more numerous electrochemical processes. The lowest energy absorption in the electronic spectrum of the bimetallic complex, $[(tpy)Ru(tpp)IrCl_3]^{2+}$, is an iridium-based transition, while the emissive state appears to be a ruthenium-based metal-to-bridging ligand charge-transfer state.

Introduction

Recognition of the photoinduced properties of $[Ru(bpy)_3]^{2+}$ stimulated further research into its properties and those of related derivatives.[1] Since that time, there has been increasing interest in the preparation and study of polymetallic ruthenium complexes containing polypyridyl bridging ligands because they can utilize intramolecular photoinitiated electron or energy transfer.[2] Polymetallic systems are also of interest as potential "electron reservoirs" for catalysis of multielectron reactions such as carbon dioxide reduction.[3] Although substantial attention has focused on the utilization of bidentate bridging ligands in homometallic systems, little work has involved the incorporation of tridentate bridging ligands.[2,4] Only recently have tridentate polypyridyl bridging ligands, such as tpp, been used in the building of polymetallic systems.[4] These systems should possess added stability over bidentate bridged systems due to the chelate effect.[6] Mixed-metal systems make possible the development of supramolecular complexes having widely varied functions at the different metal centers.

We have used the tridentate nitrogen aromatic heterocyclic ligand tpp as the bridging ligand to prepare a bimetallic ruthenium(II)/iridium(III) mixed-metal complex. The terminal ligand, tpy, is bound to the other coordination sites on the ruthenium to complete its coordination sphere, while chloride ligands occupy the additional coordination sites on the iridium metal center. This complex is the first example of a mixed-metal tpp-bridged system and contains metals which can function as both a light absorber, ruthenium, and a catalytic center, iridium.

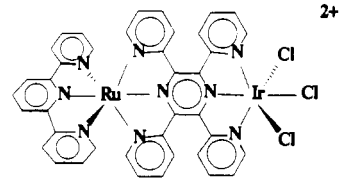

The monometallic model system $[Ir(tpp)Cl_3]$ has been crystallized and its structure determined by X-ray crystallography. Electrochemistry, emission spectroscopy, excited-state lifetime

† Current address: INC4, MS 345, Los Alamos National Laboratory, Los Alamos, NM 87545.

(1) (a) Gafney, H. D.; Adamson, A. W. *J. Am. Chem. Soc.* **1972**, *94*, 8238. (b) Navon, G.; Sutin, N. *Inorg. Chem.* **1974**, *13*, 2159. (c) Bock, C. R.; Meyer, T. J.; Whitten, D. G. *J. Am. Chem. Soc.* **1974**, *96*, 4710. (d) Bock, C. R.; Connor, J. A.; Gutierrez, A. R.; Meyer, T. J.; Whitten, D. G.; Sullivan, B. P.; Nagle, J. K. *J. Am. Chem. Soc.* **1979**, *101*, 4815. (e) Sutin, N.; Creutz, C. *Adv. Chem. Ser.* **1978**, *No. 168*, 1. (f) Meyer, T. J. *Acc. Chem. Res.* **1978**, *11*, 94. (g) Sabbatini, N.; Balzani, V. *J. Am. Chem. Soc.* **1972**, *94*, 7587. (h) Demas, J. N.; Adamson, A. W. *J. Am. Chem. Soc.* **1972**, *93*, 1800. (i) Kane-Maguire, N. A. P.; Langford, C. H. *J. Am. Chem. Soc.* **1972**, *94*, 2121. (j) Balzani, V.; Moggi, L.; Manfrin, M. F.; Bolleta, F.; Laurence, G. A. *Coord. Chem. Rev.* **1975**, *15*, 321. (k) Lin, C. T.; Bottcher, W.; Chou, M.; Creutz, C.; Sutin, N. *J. Am. Chem. Soc.* **1976**, *98*, 6536.

(2) (a) Brauenstein, C. H.; Baker, A. D.; Strekas, T. C.; Gafney, H. D. *Inorg. Chem.* **1986**, *23*, 857. (b) Rillema, D. P.; Mack, K. B. *Inorg. Chem.* **1982**, *21*, 3849. (c) Wallace, A. W.; Murphy, W. R., Jr.; Petersen, J. D. *Inorg. Chim. Acta* **1989**, *166*, 47. (d) Dose, E. V.; Wilson, L. J. *Inorg. Chem.* **1978**, *17*, 2660. (e) Hanziker, M.; Ludi, A. *J. Am. Chem. Soc.* **1977**, *99*, 7370. (f) Ruminski, R. R.; Petersen, J. D. *Inorg. Chem.* **1982**, *21*, 3706. (g) Fuchs, Y.; Lofters, S.; Dieter, T.; Shi, W.; Morgan, R.; Strekas, T. C.; Gafney, H. D.; Baker, A. D. *J. Am. Chem. Soc.* **1987**, *109*, 2691. (h) Baiano, J. A.; Carlson, D. L.; Wolosh, G. M.; DeJesus, D. E.; Knowles, C. F.; Szabo, E. G.; Murphy, W. R. *Inorg. Chem.* **1990**, *29*, 2327. (i) Denti, G.; Campagna, S.; Sabatino, L.; Scolastica, S.; Ciano, M.; Balzani, V. *Inorg. Chem.* **1990**, *29*, 4750. (j) Sahai, R.; Morgan, L.; Rillema, D. P. *Inorg. Chem.* **1988**, *27*, 3495. (k) Katz, N. E.; Creutz, C.; Sutin, N. *Inorg. Chem.* **1988**, *27*, 1687. (l) Murphy, W. R.; Brewer, K. J.; Getliffe, G.; Petersen, J. D. *Inorg. Chem.* **1989**, *28*, 81. (m) Kalyanasundaram, K.; Nazeeruddin, Md. K. *Chem. Phys. Lett.* **1989**, *158*, 45. (n) Tapolsky, G.; Duesing, R.; Meyer, T. J. *Inorg. Chem.* **1990**, *29*, 2285. (o) Rillema, D. P.; Callahan, R. W.; Mack, K. B. *Inorg. Chem.* **1982**, *21*, 2589. (p) Haim, W.; Kohlman, S. *Inorg. Chem.* **1990**, *29*, 2909. (q) Rillema, D. P.; Taghdiri, D. G.; Jones, D. S.; Keller, C. D.; Worl, L. A.; Meyer, T. J.; Levy, H. A. *Inorg. Chem.* **1987**, *26*, 578. (r) Barigelletti, F.; DeCola, L.; Balzani, V.; Hage, R.; Haasnoot, J. G.; Reedijk, J.; Vos, J. G. *Inorg. Chem.* **1989**, *28*, 4344. (s) Jaradat, G.; Barqawi, K.; Akasheh, T. S. *Inorg. Chim. Acta* **1986**, *116*, 63. (t) Ruminski, R.; Cambron, R. T. *Inorg. Chem.* **1990**, *29*, 1575. (u) Robin, M. B.; Day, P. *Adv. Inorg. Chem. Radiochem.* **1967**, *10*, 247. (v) Brewer, K. J.; Lumpkin, R. S.; Otvos, J. W.; Spreer, L. O.; Calvin, M. *Inorg. Chem.* **1989**, *28*, 4446.

0020-1669/93/1332-0898$04.00/0

measurements, UV–vis absorption spectroscopy, and spectroelectrochemistry have been used in the analysis of these systems.

Experimental Section

Materials. All chemicals were reagent grade and used without further purification. Ruthenium trichloride and iridium trichloride were received from the Johnson Matthey precious metal loan program. The ligand tpp was first prepared by Goodwin and Lions[7] and is now available commercially from GFS Chemicals. The ligand tpy was purchased from Aldrich Chemical Co. The UV grade acetonitrile and dimethylformamide solvents (Burdick and Jackson) used in the electrochemical and spectroelectrochemical experiments were dried over activated molecular sieves. All other solvents were obtained from Fisher Scientific.

Syntheses. Trichloro(2,2′:6′,2″-terpyridine)ruthenium(III) was prepared according to the published methods.[8]

Trichloro[2,3,5,6-tetrakis(2-pyridyl)pyrazine]iridium(III). [Ir(tpp)Cl_3] was prepared by adding solid $IrCl_3 \cdot 3H_2O$ (0.515 g, 0.161 mmol) to a solution of the ligand tpp (0.705 g, 0.181 mmol) in 25 mL of ethylene glycol. The solution was heated near reflux for ca. 25 min and filtered while hot. The product was washed with 60 mL of water, 60 mL of ethanol, and 75 mL of anhydrous diethyl ether. The product was dried under vacuum. A typical yield for the reaction was 45%.

(2,2′:6′,2″-Terpyridine)[2,3,5,6-tetrakis(2-pyridyl)pyrazine]ruthenium(II) Bis(hexafluorophosphate).[9] [Ru(tpy)(tpp)]$(PF_6)_2$ was prepared by adding solid Ru(tpy)Cl_3 (0.152 g, 0.345 mmol) to a solution of tpp (0.413 g, 1.06 mmol) and 1.5 mL of triethylamine in 30 mL of 2:1 (v/v) ethanol/distilled water mixture. This was heated at reflux for 5 h. The complex was precipitated by the addition of saturated, aqueous KPF_6 (20 mL) and separated by vacuum filtration. Purification was performed by column chromatography on adsorption alumina in 2:1 (v/v) toluene/acetonitrile. A typical yield for this reaction was 82%.

(2,2′:6′,2″-Terpyridine-2κ^3N,N',N'')[(μ-2,3,5,6-tetrakis(2-pyridyl)pyrazine)-1κ^3N^1,N^2,N^6:2κ^3N^3,N^4,N^5]iridium(III)ruthenium(II) Trichloride Bis(hexafluorophosphate). [(tpy)Ru(tpp)$IrCl_3$]$(PF_6)_2$ was prepared by reacting solid Ru(tpy)Cl_3 (0.150 g, 0.340 mmol) and Ir(tpp)Cl_3 (0.096 g, 0.140 mmol) in a mixture of 10 mL of dimethylformamide and 10 mL of absolute ethanol. The solution was heated at reflux for ca. 4 h. Next, the ethanol was removed by rotary evaporation. The complex was precipitated by the addition of saturated, aqueous KPF_6 (20 mL) and separated by vacuum filtration. Purification was achieved by size-exclusion column chromatography on a Sephadex LH-20 (Pharmacia) column developed with a 2:1 (v/v) ethanol/acetonitrile solvent mixture. The first band eluted was dark purple and contained the product of interest. This purification process was repeated twice, and purity was established by thin-layer chromatography. A typical yield for this reaction was 62%.

Crystal Growth and Analysis. X-ray-quality crystals of the complex [Ir(tpp)Cl_3] were obtained by recrystallization from hot dimethylformamide. A blood-red crystal obtained in this fashion with the dimensions 0.05 mm × 0.2 mm × 0.3 mm was mounted on a thin glass fiber. The lattice constants were determined by a least-squares fit of 25 reflections in the range $28° < 2\theta < 34°$. Data were collected at room temperature on a Syntex $P2_1$ instrument (upgraded to Nicolet R3 specifications) with a graphite monochromator and Mo Kα radiation (λ = 0.710 69 Å).[10] Two standard reflections (202, 004) were monitored every 96 reflections and showed no systematic variation. The intensities of 4138 reflections were measured by using a Wyckoff ω scan (0.8° range) with speeds varying 6–60°/min. All data reduction, including Lorentz, polarization, and absorption corrections, structure solution and refinement, and graphics were performed using SHELXTL 5.1 software.[11] Empirical absorption corrections, based on ψ scan data, ranged from 0.38 to 0.94. Following the data reduction, 3342 unique reflections remained with 2911, having $|F| > 3\sigma$, retained for structure solution and refinement. The positions of the Ir and Cl atoms were found via the direct methods, routine SOLV, with the nitrogen, oxygen, and carbon atoms being found from subsequent electron difference synthesis. The presence of a noncoordinated organic species was interpreted in terms of a dimethylformamide solvate. Unconstrained refinement of the C, N, O fragments was successful, although the large thermal parameters on the methyl carbon atoms indicated the presence of large vibrational motion or unresolved disorder. No residual electron density peaks greater than 0.3 e/Å^3 were observed in the region of the solvate molecule. All non-hydrogen atoms were refined anisotropically. The hydrogen atoms were refined isotropically with bond lengths fixed at 0.96 Å and isotropic thermal parameters fixed at 1.2 times the equivalent isotropic thermal parameters of the corresponding atom. Scattering factors provided by the SHELXTL package were employed. The final refinement included 201 least-squares parameters with a mean value of $|\Delta/\sigma| = 0.005$ and $g = 0.000\,16$. The goodness of fit was 1.364, and the final difference map showed a residual of 1.3 e/Å^3 near Ir. Crystallographic data may be found in Tables I–III.

Spectroscopy. Absorption spectra were recorded at room temperature in acetonitrile on a Hewlett Packard 8452 diode array spectrophotometer (resolution 2 nm).[3a]

Emission spectra were recorded at room temperature in deoxygenated acetonitrile solution and obtained on a PTI MSIII spectrofluorometer utilizing a 150-W mercury arc lamp excitation source and a thermoelectrically cooled Hamamatsu R666-S photomultiplier tube utilizing a single photon-counting detection system. Excited-state lifetime measurements were obtained on a PTI PL2300 nitrogen laser equipped with a PL201 dye laser as the excitation source. The excitation pulse passes

Table I. Crystallographic Data for [Ir(tpp)Cl_3]

chem form	$Ir(C_{26}N_6H_{16})Cl_3$	Z	4
fw	710.91	T, °C	20
space group	$C2/c$	λ, Å	0.710 69
a, Å	8.745(2)	ρ_{calcd}, g cm^{-3}	1.68
b, Å	21.215(5)	μ, cm^{-1}	154.0
c, Å	17.734(4)	transm coeff	0.376–0.938
β, deg	92.21(2)	$R(F_o)$	0.0433
V, Å^3	3288(1)	$R_w(F_o)$	0.0456

Table II. Atomic Coordinates (×10^4) and Isotropic Thermal Parameters (Å^2 × 10^3) for [Ir(tpp)Cl_3]

	x	y	z	U^a
Ir	0	8870(1)	2500	34(1)
Cl(1)	1069(2)	8869(1)	1305(1)	57(1)
Cl(2)	0	9984(1)	2500	66(1)
N(1)	0	7967(4)	2500	45(2)
C(1)	1173(6)	7656(3)	2865(3)	42(2)
C(2)	1012(7)	7005(3)	2946(3)	43(2)
N(2)	0	6693(4)	2500	46(2)
N(11)	2099(5)	8717(3)	2997(3)	46(2)
C(12)	3191(7)	9151(4)	3172(4)	55(2)
C(13)	4626(8)	8983(4)	3436(4)	64(3)
C(14)	4988(7)	8355(4)	3495(4)	61(3)
C(15)	3899(6)	7889(4)	3315(3)	50(2)
C(16)	2435(7)	8088(3)	3092(3)	46(2)
N(21)	2208(7)	6940(3)	4177(3)	58(2)
C(22)	2919(8)	6612(4)	4734(4)	64(3)
C(23)	3257(10)	5983(4)	4684(4)	75(3)
C(24)	2889(10)	5672(4)	4015(4)	75(3)
C(25)	2160(9)	6000(4)	3433(4)	62(3)
C(26)	1835(7)	6625(4)	3532(3)	51(2)
O	1600(10)	11974(5)	3254(5)	118(4)
C(30)	1684(12)	11449(7)	3488(6)	97(5)
N(30)	2522(11)	11285(4)	4100(4)	93(4)
C(31)	2741(25)	10676(7)	4390(8)	263(14)
C(32)	3219(15)	11770(9)	4546(7)	190(10)

[a] Equivalent isotropic U defined as one-third of the trace of the orthogonalized U_{ij} tensor.

(3) (a) Rasmussen, S. C.; Richter, M. M.; Yi, E.; Place, H.; Brewer, K. J. *Inorg. Chem.* **1990**, *29*, 3926. (b) Bolinger, C. M.; Sullivan, B. P.; Conrad, D.; Gilbert, J. A.; Story, N.; Meyer, T. J. *J. Chem. Soc., Chem. Commun.* **1985**, 796. (c) Bolinger, C. M.; Story, N.; Sullivan, B. P.; Meyer, T. J. *Inorg. Chem.* **1988**, *27*, 4582. (d) Bridgewater, J.; Vogler, L. M.; Molnar, S. M.; Brewer, K. J. *Inorg. Chem.*, submitted for publication.

(4) (a) Pfeiffer, F. R.; Case, F. H. *J. Org. Chem.* **1966**, *31*, 3384. (b) Ruminski, R.; Kiplinger, J.; Cockroft, T.; Chase, C. *Inorg. Chem.* **1989**, *28*, 370. (c) Petersen, J. D. Supramolecular Photochemistry. *NATO ASI Ser.* **1987**, *214*, 135. (d) Ruminski, R. R.; Letner, C. *Inorg. Chim. Acta* **1989**, *162*, 175.

(5) Berger, R. M.; McMillin, D. R. *Inorg. Chem.* **1988**, *27*, 4245.

(6) Cotton, F. A.; Wilkinson, G. *Advanced Inorganic Chemistry*, 5th ed.; John Wiley & Sons: New York, 1988; pp 45–46.

(7) Goodwin, H. A.; Lions, F. *J. Am. Chem. Soc.* **1959**, *81*, 6415.

(8) Sullivan, B. P.; Calvert, J. M.; Meyer, T. M. *Inorg. Chem.* **1980**, *19*, 1404.

(9) (a) Thummel, R. P.; Chirayil, S. *Inorg. Chim. Acta* **1988**, *154*, 77.

(10) Campana, C. F.; Shepard, D. F.; Litchman, W. M. *Inorg. Chem.* **1981**, *20*, 4039.

(11) Crystallography performed at Washington State University. Sheldrick, G. *SHELXTL*; Nicolet Analytical Instruments: Madison, WI, 1986.

Table III. Selected Bond Lengths and Bond Angles for $[Ir(tpp)Cl_3]$

	Bond Lengths (Å)		
Ir–Cl(1)	2.349(2)	Ir–Cl(2)	2.363(3)
Ir–N(1)	1.917(8)	Ir–N(11)	2.032(5)
Ir–Cl(1A)	2.349(2)	Ir–N(11A)	2.032(5)
	Bond Angles (deg)		
Cl(1)–Ir–Cl(2)	90.1(1)	Cl(1)–Ir–N(1)	89.9(1)
Cl(2)–Ir–N(1)	180.0(1)	Cl(1)–Ir–N(11)	90.4(1)
Cl(2)–Ir–N(11)	99.2(2)	N(1)–Ir–N(11)	80.8(2)
Cl(1)–Ir–Cl(1A)	180.0(2)	Cl(2)–Ir–Cl(1A)	90.1(1)
N(1)–Ir–Cl(1A)	89.9(1)	N(11)–Ir–Cl(1A)	89.6(1)
Cl(1)–Ir–N(11A)	89.6(1)	Cl(2)–Ir–N(11A)	99.2(2)
N(1)–Ir–N(11A)	80.8(2)	N(11)–Ir–N(11A)	161.5(3)
Cl(1A)–Ir–N(11A)	90.4(1)		

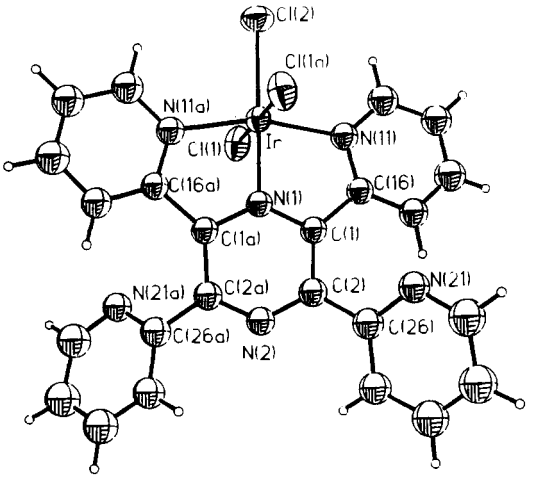

Figure 1. Diagram of $[Ir(tpp)Cl_3]$, showing thermal ellipsoids.

through an optical trigger prior to entering the sample compartment. The emission from the excited sample is detected at a right angle. The emission passes through a PTI 1200 L/mm grating monochromator and is detected by a Products For Research thermoelectrically cooled Hamamatsu R666-S photomultiplier tube. The signal from the photomultiplier tube is passed through a Calav 7901 fast amplifier into a LeCroy 6880B digitizer. The LeCroy digitizer is interfaced to a computer for data collection and analysis. The raw data were fit to a single exponential function following the removal of the initial data which included the optical delay and rise time of the system.

Electrochemistry. Cyclic voltammograms were performed on a Bio-Analytical Systems 100A electrochemical analyzer as described previously.[3a]

Spectroelectrochemistry. Electronic spectra of electrogenerated oxidation states were recorded using a cell described previously with a carbon cloth working electrode and potential control by a BAS 100B electrochemical analyzer.[3v] Oxidative spectroelectrochemistry was obtained in acetonitrile solution, while reductive spectroelectrochemistry utilized dimethylformamide as a solvent. The spectra presented in each figure are from the same solution and are presented so that relative intensity of the observed transitions is as illustrated.

Results

The title complex $[(tpy)Ru(tpp)IrCl_3]^{2+}$ can be prepared under relatively mild conditions and in reasonably good yield from the monometallic fragments $[Ru(tpy)Cl_3]$ and $[Ir(tpp)Cl_3]$. The bimetallic system exhibits five reversible redox processes and possesses a complex electronic spectrum with transitions throughout the ultraviolet and visible region of the spectrum (200–700 nm).

The iridium monometallic fragment, $[Ir(tpp)Cl_3]$, forms large blood-red crystals upon slow evaporation of a dimethylformamide solution. A diagram of $[Ir(tpp)Cl_3]$ showing thermal ellipsoids is given in Figure 1. The Ir atom has a distorted octahedral geometry. The equatorial plane is defined by the three nitrogens of the tpp ligand and a chlorine atom. Two other chlorine atoms occupy the axial positions. An axis of 2-fold symmetry bisects the tpp ligand, the Ir atom, and the equatorial Cl atom. Bond lengths and angles are given in Table III. There are two dimethylformamide molecules per $[Ir(tpp)Cl_3]$ in the crystal lattice. The coordinated pyridine rings make an angle of 33.4° with the pyrazine ring. Atomic coordinates are given in Table II with bond lengths and angles given in Table III.

Table IV. Cyclic Voltammetric Data for a Series of Iridium(III) and Ruthenium(II) Complexes Incorporating Tridentate Polypyridyl Bridging Ligands

complex	$E_{1/2}$, V	assgnt
$[Ir(tpp)Cl_3]$	+1.17	Ir(III)/Ir(IV)
	−0.78	tpp/tpp^-
	−1.35	Ir(III)/Ir(I)
$[Ru(tpy)(tpp)]^{2+}$	+1.40	Ru(II)/Ru(III)
	−0.97	tpp/tpp^-
	−1.38	tpy/tpy^-
	−1.60	tpp^-/tpp^{2-}
$[(tpy)Ru(tpp)IrCl_3]^{2+}$	+1.92	Ir(III)/Ir(IV)
	+1.56	Ru(II)/Ru(III)
	−0.29	tpp/tpp^-
	−0.83	tpp^-/tpp^{2-}
	−1.42	tpy/tpy^-

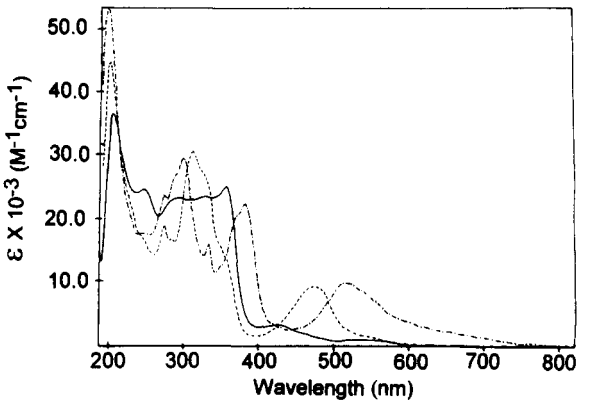

Figure 2. Electronic absorption spectra for iridium(III) and ruthenium(II) complexes incorporating a tridentate polypyridyl bridging ligand: (—) $[Ir(tpp)Cl_3]$; (- - -) $[Ru(tpy)(tpp)]^{2+}$; (· · ·) $[(tpy)Ru(tpp)IrCl_3]^{2+}$.

The electrochemical data for the two monometallic and the title bimetallic complex are given in Table IV. The complex $[Ir(tpp)Cl_3]$ exhibits one oxidative and two reductive waves. The oxidative process is quasi-reversible (i_p^a/i_p^c = 0.9). The first reductive process is reversible (i_p^a/i_p^c = 1.0), while the second reduction is totally irreversible at scan rates below 10 V/s. This second reduction is followed by a chemical reaction of the electrogenerated $[Ir(tpp)Cl_3]^{2-}$.

The complex $[Ru(tpp)(tpy)]^{2+}$ exhibits one reversible oxidative and three reversible reductive waves.

The bimetallic system, $[(tpy)Ru(tpp)IrCl_3]^{2+}$, gives two reversible oxidations and three reversible reductions.

The absorption spectra for $[Ir(tpp)Cl_3]$, $[Ru(tpy)(tpp)]^{2+}$, and $[(tpy)Ru(tpp)IrCl_3]^{2+}$ are shown in Figure 2. The lowest energy absorption bands show a solvent dependence of the absorption maximum shifting to lower energies in solvents with lower dielectric constants. All of the complexes studied emit in fluid solution at room temperature.

Electrogeneration of many different oxidation states of these ruthenium monometallic and ruthenium/iridium bimetallic systems was possible. Electronic spectroscopy of these complexes in all stable oxidation states has been performed, and the results of these spectroelectrochemical studies are shown in Figures 3 and 4.

Discussion

X-ray Crystallography. As can be seen from the bond distances and angles given in Table III, the geometrical constraints of the

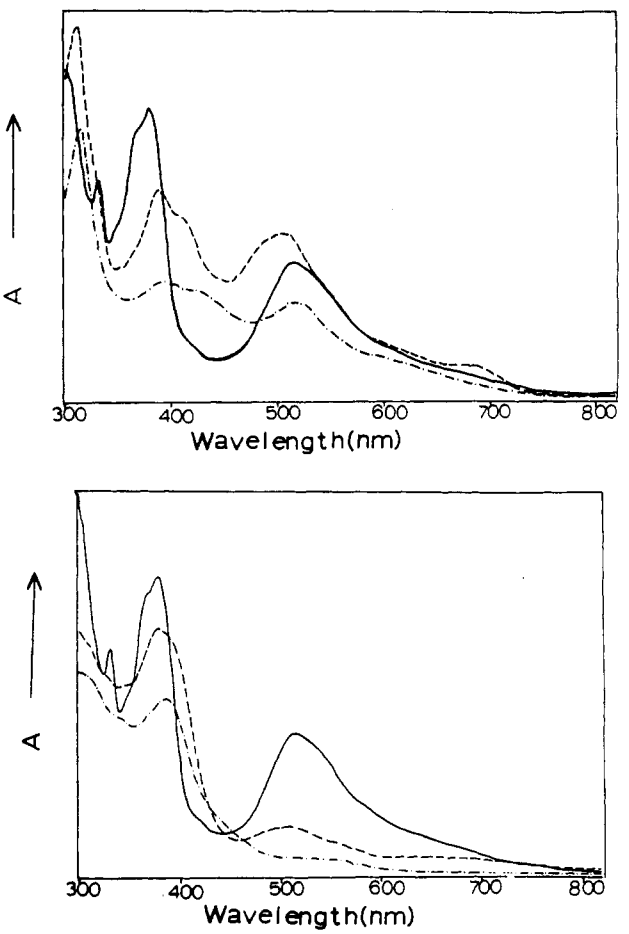

Figure 3. Spectroelectrochemical results for $[(tpy)Ru(tpp)IrCl_3]^{2+}$: (a, top) (—) original oxidation state, (- - -) 1-electron reduction, (- · -) 2-electron reduction; (b, bottom) (—) original oxidation state, (- - -) 1-electron oxidation, (- · -) 2-electron oxidation.

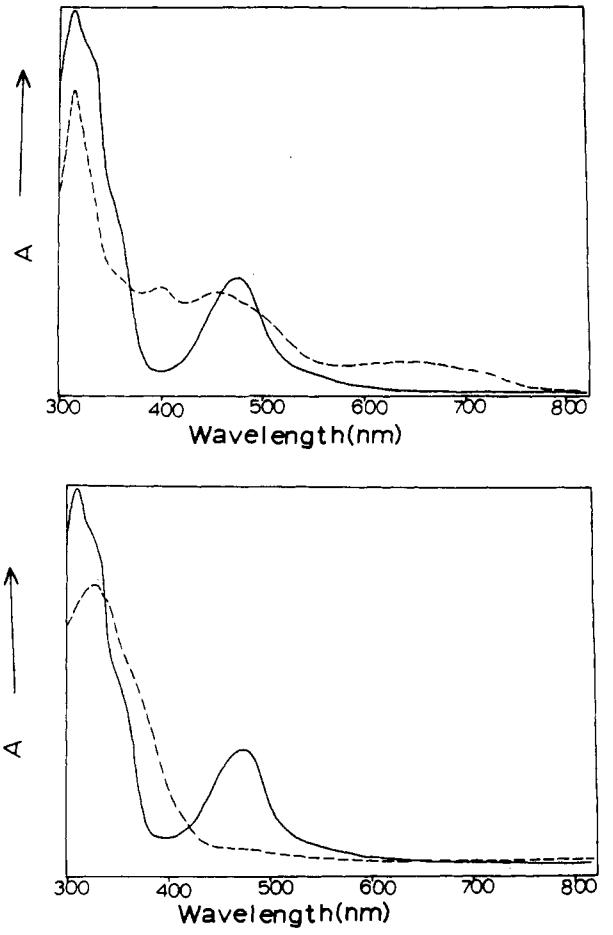

Figure 4. Spectroelectrochemical results for $[Ru(tpp)(tpy)]^{2+}$: (a, top) (—) original oxidation state, (- - -) 1-electron reduction; (b, bottom) (—) original oxidation state, (- - -) 1-electron oxidation.

tpp ligand cause a distortion from octahedral coordination. The "bite" angle of tridentate diimine ligands, such as tpp, gives rise to bond angles less than ideal as illustrated by the N(1)–Ir–N(11) angle of 80.8(2)° and differing metal to nitrogen bond distances within the tpp ligand.

Examination of the conformation of the coordinated tpp ligand within the $[Ir(tpp)Cl_3]$ framework shows large distortions from planarity. The four pyridine rings are not expected to be coplanar due to steric repulsions that would be present between ring hydrogens on the 3-pyridyl positions. This repulsion can be alleviated by the rotation of the two uncoordinated pyridine rings. For this reason, it is somewhat surprising that the two coordinated pyridine rings are 33.4° out-of-plane with respect to the pyrazine ring in tpp. In addition, the pyrazine ring itself exhibits some degree of torsion, possibly due to the movement of the attached pyridine rings. This lack of planarity of the pyrazine ring is expected to have marked effects on the metal–metal communication in polymetallic systems bridged through this tpp ligand.

Work is currently in progress in our laboratory to synthesize the tridentate bridging ligand tetrapyrido(2,3-*a*:3′,2′-*c*:2″,3′-*h*:3‴,2‴-*j*)phenazine (tpph) shown as follows:[4]

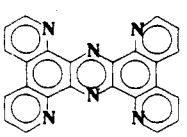

Formation of these carbon–carbon bonds between the 3-positions on the pyridine rings of the tpp ligand will help minimize the twisting of the pyridine rings. This will hopefully limit distortions from planarity in the pyrazine ring and therefore provide better metal–metal communication in multimetallic systems.

Electrochemistry. All the complexes studied possess numerous electroactive moieties. In general, reversible reductive processes in complexes of this type will be ligand localized, due to the presence of low-lying π^* orbitals on these polypyridyl systems.[2,4] Totally irreversible electrochemical reductions are often observed for systems containing iridium(III). These processes are normally irreversible two electron metal-based reductions which result in the generation of an iridium(I) d^8 system. This d^8 species rearranges from an octahedral to a square planar ligand environment by loss of two chloride ligands.[3a,12] Oxidations observed for ruthenium or iridium polypyridyl complexes are metal-based processes and are usually reversible on the cyclic voltammetric time scale.[2,4,9,12] The cyclic voltammetric data for these systems are given in Table IV with peak assignments included.

The monometallic ruthenium complex has been previously prepared and the electrochemistry studied.[9] The half-wave potentials given are for our sample studied under our conditions for comparison. The oxidation at +1.40 V has previously been assigned a Ru(II)/Ru(III) metal-based process, and the first reduction at −0.97 V, as a tpp-based reduction.[9] The second wave at −1.38 V is assigned as a tpy reduction. The third reduction at −1.60 V is assigned as a second tpp-based reduction (tpp^-/tpp^{2-}) on the basis of the reductions observed in the free tpp and tpy ligands.[4]

(12) (a) DeArmond, K.; Hillis, J. *J. Chem. Phys.* **1971**, *54*, 2247. (b) Kahl, J. L.; Hanck, W.; DeArmond, M. K. *J. Phys. Chem.* **1978**, *82*, 540.

The quasi-reversible oxidation of $[Ir(tpp)Cl_3]$ at +1.17 V is assigned as an Ir(III)/Ir(IV) metal-based process. The first-reduction at –0.78 V is assigned as a ligand (tpp) based reduction. The second reduction at –1.35 V is irreversible and assigned as an Ir(III)/Ir(I) metal-based process.

In the bimetallic system, one would expect to see a sum of all the electrochemical processes observed in the monometallic fragments $[Ir(tpp)Cl_3]$ and $[Ru(tpy)(tpp)]^{2+}$ with perturbations introduced by the formation of the bridged system. The stabilization of the bridging ligand based π^* orbitals upon formation of a bimetallic system often gives rise to two sequential one-electron reductions of the bridging ligand prior to reduction of other electroactive moieties.[2,9] The first two reductions at –0.29 and –0.83 V are assigned as sequential one-electron reductions of the tpp ligand, and the third reduction at –1.42 V is assigned as a tpy ligand-based reduction. The iridium-based reduction displayed by the $[Ir(tpp)Cl_3]$ system is not seen in the bimetallic complex. This is due to the fact that the two tpp-based and the one tpy-based reductions occur at lower potentials than the iridium-based process. Therefore, the iridium metal center will be more electron rich prior to its reduction due to the coordination to a doubly reduced tpp ligand. This will shift the iridium reduction beyond the solvent window.

The oxidations in the bimetallic complex are metal-based processes with the one at +1.92 V assigned as an Ir(III)/Ir(IV) oxidation and the one at +1.56 V being assigned as a Ru(II)/Ru(III) oxidation primarily on the basis of the spectroelectrochemistry results. As reported previously,[9] a slight shift would be expected for the ruthenium-based oxidation in the bimetallic system as compared to the monometallic due to the electron-withdrawing effect of the additional metal center upon formation of the bimetallic complex and the enhanced π back-bonding ability of the tpp ligand. A large shift is observed for the Ir(III)/Ir(IV) oxidation in the bimetallic as compared to the monometallic due to the addition on the Ru^{II}tpy moiety as well as the additional 1+ charge added to the molecule by the presence of the ruthenium-based oxidation, which occurs prior to this iridium-based process.

Electronic Absorption Spectroscopy. The mixed-ligand complex, $[Ru(tpy)(tpp)]^{2+}$, has a complicated spectrum consisting of both ligand-based $\pi \rightarrow \pi^*$ and metal-to-ligand charge-transfer (MLCT) bands. The lowest energy absorption at 472 nm shows solvent-dependent behavior consistent with a MLCT assignment.[13] The free ligand spectrum of tpp has absorptions at 274 and 308 nm whereas the tpy absorptions are at 236 and 278 nm. The electrochemical data for this system indicate that both tpp- and tpy-based π^* orbitals are present at relatively low energy. The band at 472 nm can be assigned as two overlapping MLCT transitions, $Ru(d\pi) \rightarrow tpp(\pi^*)$ and $Ru(d\pi) \rightarrow tpy(\pi^*)$, with the tpp-based MLCT occurring at slightly lower energy.[9] Both tpp and tpy ligand-based $\pi \rightarrow \pi^*$ bands are observed in the ultraviolet with the tpy peak maximum at 310 nm, while the tpp transitions appear as shoulders at 328 and 354 nm.[2] Higher energy MLCT transitions based on each ligand occur as shoulders on the ligand-based $\pi \rightarrow \pi^*$ bands observed in the ultraviolet.[2,9]

The monometallic iridium system, $[Ir(tpp)Cl_3]$, displays a series of transitions throughout the ultraviolet and visible region of the spectrum. The lowest energy band at 558 nm as well as the more intense band at 424 nm exhibit a solvent dependence consistent with an assignment as a MLCT transitions.[13] Due to the significant amount of spin–orbit coupling observed for iridium systems, transitions which are normally spin forbidden, such as ^{3}MLCT transitions, can be observed in the electronic spectrum. Therefore, the lowest energy band at 558 nm is assigned as an Ir → tpp ^{3}MLCT, while the more intense band at 424 nm is assigned as the Ir → tpp ^{1}MLCT transition. A less intense transition at 498 nm is also observed and may represent another ^{3}MLCT transition. The remaining peaks in the ultraviolet region of the spectrum are assigned to ligand-localized $\pi \rightarrow \pi^*$ transitions on the basis of their extinction coefficients and their similarity to transitions observed in the free ligands and by analogy to the previously studied rhodium analogue, $[Rh(tpp)Cl_3]$.[4,9] The lowest lying tpp-based $\pi \rightarrow \pi^*$ transition occurs at 370 nm. This is significantly lower than the analogous transition in the ruthenium monometallic system, which occurs at 328 nm. The lower energy of this transition is consistent with the decreased back-bonding ability of the Ir(III) metal center.

On the basis of the absorptions observed for the monometallic systems, we can assign the transitions seen in the mixed-metal bimetallic complex. The broad peak seen in the visible region of the spectrum between 480 and 630 nm is composed of many transitions. By analogy to the monometallic fragments, the lowest energy component at ca. 660 nm, which has a relatively low extinction coefficient, can be assigned as the $Ir(d\pi) \rightarrow tpp(\pi^*)$ ^{3}MLCT transition. The intense portion of this peak between 480 and 610 nm is expected to contain two ^{1}MLCT bands. These include the $Ru(d\pi) \rightarrow tpp(\pi^*)$ ^{1}MLCT and the $Ir(d\pi) \rightarrow tpp(\pi^*)$ ^{1}MLCT. Both the ruthenium and iridium bridging ligand based MLCT bands should shift to lower energy upon formation of the bimetallic complex.[2,9] The magnitude of this shift is expected to be greater for ruthenium than for iridium; therefore, the relative ordering of the bridging ligand based MLCT transitions should not change upon the formation of the bridged system. The lowest energy component of these overlapping ^{1}MLCT bands should be the $Ru(d\pi) \rightarrow tpp(\pi^*)$ transition. In the bimetallic complex, the ruthenium back-bonding to the bridging ligand is reduced. This will give rise to enhanced back-bonding to the tpy in the bimetallic complex as compared to the ruthenium monometallic system. This should give rise to a blue shift of the Ru → tpy MLCT. Thus the shoulder observed at 425 nm in the bimetallic system is assigned as the $Ru(d\pi) \rightarrow tpy(\pi^*)$ ^{1}MLCT. The intense peaks in the ultraviolet region show very little solvent dependence and are assigned as ligand-based $\pi \rightarrow \pi^*$ transitions for both tpp and tpy. It is interesting to note that the lowest lying tpp-based $\pi \rightarrow \pi^*$ transitions occurs at 380 nm in the bimetallic complex, consistent with a stabilization of the π^* orbitals upon complexation of two metal centers. Shoulders are present on these $\pi \rightarrow \pi^*$ bands due to the additional higher energy MLCT transitions.[2,9]

Spectroelectrochemistry. The spectroelectrochemistry of $[(tpy)Ru(tpp)IrCl_3]^{2+}$ and $[Ru(tpp)(tpy)]^{2+}$ is shown in Figures 3 and 4. The spectra reported in each Figure 3a,b or 4a,b are obtained from the same solution, and relative intensities for the transitions are as illustrated. Electrogeneration of the one electron oxidized or reduced form of both the bimetallic and Ru monometallic is possible with >95% regeneration of the original oxidation state. For the bimetallic, regeneration after the two-electron oxidation or reduction was possible with >80% efficiency. In the oxidative spectroelectrochemistry for the Ru monometallic, Figure 4b, the Ru → tpp and Ru → tpy MLCT transitions are completely lost upon the one-electron oxidation of the ruthenium metal. In the one-electron oxidation of the bimetallic system, Figure 3b, a loss of the ruthenium-based metal-to-ligand charge-transfer transitions (425 and 500–580 nm) is observed with no change in intensity of the iridium-based processes (600–700 nm). This observation is consistent with a ruthenium-based oxidation and inconsistent with an iridium-based process. It is interesting to note that the visible portion of the spectrum for the one electron oxidized form of the bimetallic is quite similar to the iridium monometallic $[Ir(tpp)Cl_3]$, with the transitions in the mixed-metal system being shifted to lower energy due to stabilization of the π^* orbitals on the tpp. When both metals are oxidized, all of the transitions in the 500–700-nm region are lost due to their MLCT nature. The

(13) (a) Lever, A. B. P. *Inorganic Electronic Spectroscopy*, 2nd ed.; Elsevier: Amsterdam, 1984. (b) Shoup, M.; Hall, B.; Ruminski, R. R. *Inorg. Chem.* **1988**, *27*, 200. (c) Kober, E. M.; Sullivan, B. P.; Meyer, T. J. *Inorg. Chem.* **1984**, *23*, 2098.

oxidative spectroelectrochemistry of the bimetallic system shows a loss of the transitions at 332 and 368 nm when both metals are oxidized indicating their MLCT nature.

In Figures 3a and 4a the reductive spectroelectrochemistry is shown. As expected, there is a decrease in intensity at 330 nm in the monometallic ruthenium complex as the tpp is reduced by one electron, Figure 4a. This confirms our assignment of this peak as a tpp-based $\pi \rightarrow \pi^*$ transition. Some intensity remains after the tpp is reduced due to an overlap with tpy-based transitions. When tpp is reduced, new tpp-based $\pi^* \rightarrow \pi^*$ transitions appear in the visible. This somewhat obscures the changes observed for MLCT transitions in this region. In $[Ru(tpp)(tpy)]^{2+}$, the Ru $\rightarrow$ tpy MLCT shifts to lower energy upon reduction by one electron. This is a result of tpp's diminished back-bonding ability giving rise to a electron-rich ruthenium which decreases the Ru–tpy energy gap, shifting the transition to 500 nm. At lower energy (660–730 nm) there is a band that appears in the spectra of the one electron reduced Ru monometallic. This transition most likely represents a ligand-to-metal charge-transfer (LMCT) transition (tpp $\rightarrow$ Ru). On the basis of the spectroelectrochemical assignments for the ruthenium monometallic, the transitions for $[(tpy)Ru(tpp)IrCl_3]^{2+}$ can be assigned. The transition at 390 nm that disappears when the tpp is reduced can be assigned as a tpp $\pi \rightarrow \pi^*$ transition. The two shoulders at 332 and 368 nm also appear to be lost upon tpp reduction. Combination of this result with their loss upon metal oxidation indicates that these transitions most likely represent higher energy M $\rightarrow$ tpp MLCTs. As in the ruthenium monometallic, the Ru $\rightarrow$ tpy MLCT transition shifts to lower energy in the bimetallic with reduction of the tpp. New transitions involving the redox orbital appear in the spectra of the reduced bimetallic system between 350 and 550 nm. The new band present in the singly reduced complex between 680 and 720 nm can be assigned as a tpp $\rightarrow$ Ru LMCT transition.

Emission Spectroscopy and Excited-State Lifetimes. For polypyridyl complexes of this type, visible light absorption is usually dominated by MLCT excited states which are largely singlet in character, ^{1}MLCT ($d\pi \rightarrow \pi^*$), while emission occurs from MLCT states which are largely triplet in character.[2,9,14]

$[Ir(tpp)Cl_3]$ and $[Ru(tpy)(tpp)]^{2+}$ both emit from ^{3}MLCT excited states based on the tpp ligand,[4,9] with a λ^{em}_{max} at 632 nm (τ = 1310 ns) and 670 nm (τ = 30 ns), respectively. There is a reverse in the trends of the lowest lying absorption maxima versus emission energies due to the lowest energy band in the absorption spectra being a ^{3}MLCT transition for the iridium system and a ^{1}MLCT for the ruthenium monometallic complex.[4,9] Comparison of the energy of the ^{1}MLCT of the iridium system (23.6×10^3 cm^{-1}) to the energy of the ^{1}MLCT of the ruthenium system (21.2×10^3 cm^{-1}) illustrates that the energy of the ruthenium ^{1}MLCT absorption is lower than that of the iridium ^{1}MLCT. The bimetallic system emits with a λ^{em}_{max} = 810 nm (τ = 22 ns).

On the basis of the monometallic emissions, one would expect the emitting state in the mixed-metal bimetallic system to be the ^{3}MLCT Ru($d\pi$) $\rightarrow$ tpp(π^*) excited state. The relatively short excited-state lifetime of this complex is consistent with a ruthenium- and inconsistent with an iridium-based emission. The shift of the emission maxima in the bimetallic system to lower energy than in the ruthenium monometallic system is due to a stabilization of the π^* orbital upon formation of the bimetallic complex and is similar in magnitude to the shift observed for the homometallic system, $\{[(tpy)Ru]_2(tpp)\}^{4+}$.[2,9]

The lowest energy absorption in the electronic spectrum of the bimetallic complex, $[(tpy)Ru(tpp)IrCl_3]^{2+}$, is an iridium-based ^{3}MLCT transition, while the emissive state appears to be a ruthenium-based ^{3}MLCT excited state. Excitation into either the Ir($d\pi$) $\rightarrow$ tpp(π^*) ^{3}MLCT or Ru($d\pi$) $\rightarrow$ tpp(π^*) ^{1}MLCT gives rise to the same emission centered at 810 nm, indicating communication between these states and the ruthenium-based ^{3}MLCT emitting state.

Conclusions

The use of spectroelectrochemical measurements in this mixed-metal system and the related monometallic complex has proven very useful in the elucidation of the nature of the electrochemical processes and the spectroscopic properties of these systems. The long lifetime of $[Ir(tpp)Cl_3]$ in the presence of an apparent large degree of spin–orbit coupling is quite interesting. Similar effects have been observed in our laboratory for osmium complexes containing tpp and may be a result of the restricted vibrational motion of the tridentate chelating ligand.[15] It appears from the emission studies that the tpp ligand provides excellent communication between MLCT states centered on different metals.

Further investigation of the spectroscopic, electrochemical, spectroelectrochemical, and photochemical properties of this tpp-bridged bimetallic system and substituted analogues should yield further insight into the ground- and excited-state properties of tpp-bridged mixed-metal systems.[16]

Acknowledgment. Special thanks are expressed to Prof. Roger Willett for his assistance in the determination of the crystal structure as well as to Kevin Neville for the determination of the excited-state lifetimes reported herein. The helpful comments of a reviewer of the manuscript are greatly appreciated. The X-ray diffraction facility at Washington State University was established through funds provided by NSF Grant CHE-8408407 and The Boeing Co. We also thank Johnson Matthey for the generous loan of the iridium and ruthenium metals used in this study. This work was supported in part by funds from Virginia Polytechnic Institute and State University, Washington State University, and the National Science Foundation (Grant CHE-9108374).

Supplementary Material Available: Tables 1S–6S, giving X-ray data collection parameters, atomic coordinates, bond lengths and angles, anisotropic thermal parameters, and H-atom coordinates, and Figures 1S and 2S, showing packing diagrams (8 pages). Ordering information is given on any current masthead page.

(14) (a) Berger, R. M. *Inorg. Chem.* **1990**, *29*, 1920. (b) Braunstein, C. H.; Baker, A. D.; Strekas, T. C.; Gafney, H. D. *Inorg. Chem.* **1984**, *23*, 857. (c) Carlson, D. L.; Murphy, W. R. *Inorg. Chem. Acta* **1991**, *181*, 61. (d) Murphy, W. R. Private communication. (e) Meyer, T. J. *Pure Appl. Chem.* **1986**, *58*, 9, 1193.

(15) Brewer, R. G.; Brewer, K. J. *Inorg. Chim. Acta* **1993**, manuscript in preparation.

(16) Vogler, L. M.; Brewer, K. J. Work in progress.